

Fractional quantum Hall physics in rotating ultracold Rydberg gases

F. Grusdt^{1,2} and M. Fleischhauer¹

¹*Department of Physics and research center OPTIMAS, University of Kaiserslautern, Germany*

²*Graduate School Materials Science in Mainz, Staudinger Weg 9, 55128 Mainz, Germany*

(Dated: October 1, 2012)

We study ultracold Rydberg-dressed Bose gases subject to artificial gauge fields in the fractional quantum Hall (FQH) regime. The characteristics of the Rydberg interaction gives rise to interesting many-body ground states different from standard FQH physics in the lowest Landau level (LLL). The non-local but rapidly decreasing interaction potential favors crystalline ground states for very dilute systems. While a simple Wigner crystal becomes energetically favorable compared to the Laughlin liquid for filling fractions $\nu < 1/12$, a correlated crystal of composite particles emerges already for $\nu \leq 1/6$. The presence of a new length scale, the Rydberg blockade radius a_B , gives rise to a bubble crystal phase when the average particle distance becomes less than a_B and $\nu \lesssim 1/4$. For larger fillings indications for strongly correlated cluster liquids are found.

In the context of the fractional quantum Hall effect (FQHE) interesting many body ground states exists, some of which carry fractional and non-abelian braiding statistics [1–5]. This makes them ideal candidates for a topological quantum computer [6, 7] and gives access to topological quantum phases [8]. For an experimental study a high degree of control is required and quasi-2D ultracold gases of atoms in artificial magnetic fields have been suggested as potential candidates [9]. Effective magnetic fields are generated either by rotation [10, 11] or by using light-induced gauge potentials [12–14]. When a weakly interacting superfluid Bose gas is rotated sufficiently fast an ordered vortex-lattice forms [15, 16] and the lowest Landau level (LLL) regime can be reached [17]. Although there is no integer quantum Hall effect based on the Pauli principle for bosonic atoms, repulsive interactions can give rise to highly correlated FQH states for fillings $\nu \lesssim 6$ [9] when only the LLL is occupied [18–20]. However, despite the experimental progress strongly correlated phases have not been realized yet, which can partially be attributed to the rather small interaction energies in atomic gases. In the present paper we propose an alternative using $1/r^6$ van-der-Waals (vdW) interactions in Rydberg states. The associated energies can be orders of magnitude larger than those achievable with contact or magnetic dipole-dipole interactions. We theoretically analyze the phase diagram in the LLL using exact diagonalization (ED) as well as variational methods. Similar to dipolar gases with $1/r^3$ interaction, which have been extensively studied in the past [21–23], we find a transition from Laughlin (LN) liquids [24] to crystalline ground states for very dilute systems, however with an extended filling region where only composite particles can crystallize at zero temperature. Additionally the presence of a new length scale, the Rydberg blockade radius gives rise to a clustering mechanism supporting bubble crystal ground states.

Recently there has been a lot of interest in atoms excited to high Rydberg states and there has been considerable experimental progress to make these systems accessible [25–31]. Of particular interest in the present context are atoms excited by far-off resonant laser radia-

tion. In this case, called Rydberg dressing (see fig.1 (a)), the atoms essentially remain in their ground state but show an effective interaction [32, 33]

$$V(r) = \frac{\tilde{C}_6}{a_B^6 + r^6}, \quad a_B = \left(\frac{C_6}{2\hbar\Delta} \right)^{1/6}. \quad (1)$$

For large particle separations r the interaction potential is of vdW type $\sim r^{-6}$, where $\tilde{C}_6 = (\Omega/2\Delta)^4 C_6$ describes the effective interaction strength of Rydberg dressed atoms with C_6 being the bare vdW coefficient, $\Omega \ll |\Delta|$ the Rabi-frequency of the laser excitation and Δ its detuning. Since bare Rydberg interaction energies are typically many orders of magnitude stronger than e.g. magnetic dipole-dipole interactions, the excitation gap of FQH states can easily reach the energy separation between Landau levels (LLs, see supplementary material for specific data). Most importantly the interaction potential (1) flattens off below the blockade radius a_B , thereby defining a new characteristic length scale.

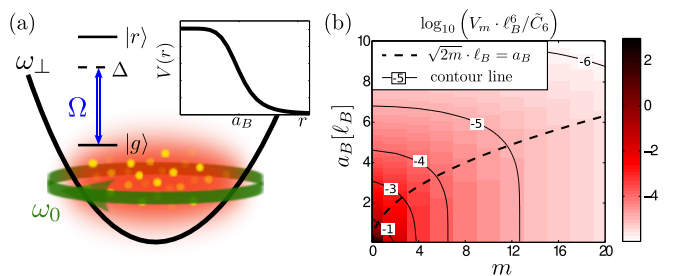


FIG. 1. (color online). (a) An ultra-cold Bose gas is dressed with Rydberg-excitations $|r\rangle$ by illuminating with a far off-resonant (detuning Δ) laser beam Ω . Rotating the gas with frequency ω_0 and applying a weak harmonic trap ω_\perp in radial and a tight one in the transverse direction ($\omega_z \gg \omega_\perp$) the quasi-2D FQH regime can be reached. (b) Contour plot of pseudopotentials V_m for the potential (1), where m was treated as continuous parameter for better illustration. Black solid lines denote contours of constant (continuous) pseudopotential.

When a Rydberg-dressed Bose gas is set into rotation with angular frequency ω_0 in a radial trap of frequency ω_\perp , the corresponding length scale is given by $\ell_c = (2m_a\sqrt{\omega_0^2 + \omega_\perp^2}/\hbar)^{-1/2}$ [34] with m_a the atomic mass. As will be shown the competition of the two length scales ℓ_c and a_B leads to interesting new physics. Already in the mean-field regime where the rotation frequency is well below the deconfinement limit ($\omega_\perp > \omega_0$) there is e.g. a competition between a vortex-lattice and a super-solid phase [35]. Here we are interested in the regime of strong correlations. To this end we consider a Rydberg-dressed Bose gas in the LLL regime for fillings $\nu < 1$, assume a quasi-2D gas, neglecting finite-thickness effects and use $\omega_\perp = \omega_0$ ($\ell_c \rightarrow \ell_B$: *magnetic* length). For simplicity we consider only even values of $1/\nu$ corresponding to bosonic LN states.

The interaction projected to the LLL is described by Haldane's two-particle pseudopotentials V_m [36], where the integer m denotes the relative angular momentum. For the interaction (1) they are plotted in fig.1(b). At given a_B the first V_m are approximately equal until the radial extend $R_m = \sqrt{2m}\ell_B$ of the wavefunction in the relative coordinate is $\sim a_B$. The subsequent pseudopotentials decrease quickly. Specific numbers are given in the supplementary material. The two regions, separated by the curve $\sqrt{2m}\ell_B = a_B$ give rise to qualitatively different physics. We first consider the case of a small blockade radius, where its effect can be disregarded.

The $\nu = 1/2$ and $\nu = 1/4$ ground states. For $a_B/\ell_B \rightarrow 0$ the first two pseudopotentials diverge

$$V_0 \approx \frac{3}{8} \frac{\tilde{C}_6}{\ell_B^6} \left(\frac{\ell_B}{a_B} \right)^4, \quad V_2 \approx \frac{1}{26} \left(0.571 - \ln \frac{a_B}{\ell_B} \right) \frac{\tilde{C}_6}{\ell_B^6}, \quad (2)$$

while all $V_{m>2}$ converge. Therefore, the $\nu = 1/2, 1/4$ bosonic LN states are exact ground states. ED calculations in spherical geometry for small particle numbers N confirm this for small but finite values of a_B/ℓ_B : even for $a_B/\ell_B = 2$ we find large overlaps squared to the LN states, being 0.992 for $\nu = 1/2$ ($N = 10$) and 0.974 for $\nu = 1/4$ ($N = 7$).

Ground states at small fillings $\nu < 1/4$. Now we want to address the physics for small fillings, i.e. $\nu < 1/4$, again for $a_B \lesssim \ell_B$. Due to the non-local interaction a natural ground state candidate in this regime is the noncorrelated Wigner crystal (NWC) [37] described by the wavefunction

$$\psi_{\text{NWC}}(z) = \mathcal{S} \prod_j e^{-(|z_j - R_j|^2 + z_j R_j^* - z_j^* R_j)/4}, \quad (3)$$

where $R_j \in \mathbb{C}$ defines a lattice in the plane of complex coordinates $z_j = (x_j + iy_j)/\ell_B$ and \mathcal{S} stands for complete symmetrization. To see if the NWC could be a ground state we compare the corresponding variational energy per particle ϵ_{NWC} to that of the LN state. To this end we generalize the expression for ϵ_{NWC} derived in [37] to

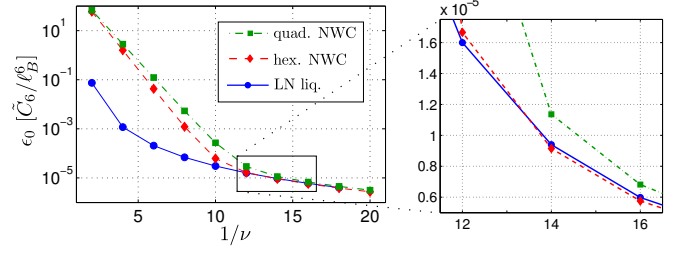


FIG. 2. (color online). Comparison of the variational energies per particle ϵ_0 (at fillings $\nu = 1/2, 1/4, 1/6, \dots$ corresponding to the bosonic Laughlin states) for the different trial wavefunctions at $a_B = 0.2\ell_B$ (LN - Laughlin states, NWC - non-correlated Wigner crystal of bare particles.)

bosons:

$$\epsilon_{\text{NWC}} = \frac{1}{2} \frac{\tilde{C}_6}{\ell_B^6} \sum_{j \neq 0} \frac{e^{-|R_j|^2/4}}{1 + \frac{1}{2}e^{-|R_j|^2/2}} \cdot K(\xi = |R_j|), \quad (4)$$

$$K(\xi) = \int_0^\infty \frac{dr r e^{-r^2/4}}{r^6 + (a_B/\ell_B)^6} \left(I_0\left(\frac{r\xi}{2}\right) + J_0\left(\frac{r\xi}{2}\right) \right),$$

where I_0, J_0 denote Bessel functions. The integral can be handled numerically and the lattice sum can easily be performed. Like for electrons [37, 38] and dipolar fermions [39], the hexagonal lattice minimizes the NWC energy, see fig.2.

In fig.2 the energies of different NWCs and the LN liquid are plotted for small $a_B = 0.2\ell_B$ and even values of $1/\nu$. The latter was calculated using the standard plasma analogy [24] for $N = 100$ particles for all examined ν with Metropolis Monte Carlo (MC) [40]. We find a transition from LN to a NWC at $\nu = \nu_{\text{NWC}} = 1/14$, although for $\nu = 1/12$ the energy difference is so small that we can not exclude a transition here. This critical filling is far below the value of $\nu \approx 1/7$ for pure Coulomb and dipolar interacting fermions [38, 39, 41].

On the other hand a simple stability analysis shows that the lattice is expected to melt only for fillings $\nu \geq \nu_{\text{Ld}} = 1/4$. Specifically we calculated the Lindemann parameter $\gamma \equiv \sqrt{\langle \delta \mathbf{u}^2 \rangle}/a$ from the phonon spectrum in harmonic and nearest-neighbor approximation following [42], where a denotes the (hexagonal) lattice constant and $\delta \mathbf{u}$ the atomic displacement from the lattice $\{R_j\}$. The phenomenological Lindemann criterion states that the crystal melts when γ exceeds a critical value γ_c . In our case $\gamma = 0.57\sqrt{\nu}$ for $a_B < \ell_B$ at zero temperature, and $\gamma_c \approx 0.28$ [39, 43]. Thus the crystal is expected to melt only for $\nu \geq 1/4$, similar to the result found in dipolar systems [22, 39]. This value differs from the transition point to a NWC, $\nu_{\text{NWC}} = 1/14$, found previously. Instead of a NWC the ground state in the region $\nu_{\text{Ld}} \leq \nu \leq \nu_{\text{NWC}}$ can however be a crystal of composite particles (CPs) [44], termed *correlated*

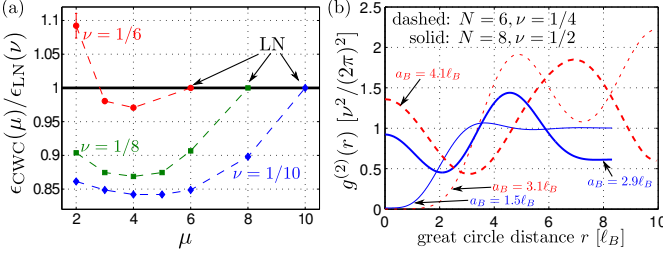


FIG. 3. (color online). (a) Variational energy per particle of the hexagonal CWC of ${}^\mu\text{CP}$, $\epsilon_{\text{CWC}}(\mu)$, in units of the LN state energy $\epsilon_{\text{LN}}(\nu)$ at filling ν . Results were obtained in Metropolis MC simulations with $N = 91$ particles. (b) Second order correlation function of the ground state for vdW interactions for $N = 8$ solid ($N = 6$ dashed) at $\nu = 1/2$ ($\nu = 1/4$). For large a_B symmetry is broken ($L \neq 0$, thick lines), in contrast to small a_B ($L = 0$, thin lines).

Wigner crystal (CWC) [45, 46]. As for the LN states the first pseudopotentials are screened for CPs and only the effects of the long-range tails of the repulsive interaction potential remain. As the latter should be the same for CPs as for bare particles the stability arguments given above remain valid and a CWC should form already for $\nu < \nu_{\text{Ld}} = 1/4$.

CWC variational wavefunctions of the form [6]

$$\psi_{\text{CWC}}^{(\mu)}(z) = \mathcal{P}_{\text{LLL}} \prod_{j < k} (z_j - z_k)^\mu \psi_{\text{NWC}}(z)$$

were investigated in [45] using plasma analogy based MC simulations, and the critical filling $\nu \approx 1/7$ in electronic systems was correctly predicted. Here \mathcal{P}_{LLL} is a projector to the LLL and $(z_j - z_k)^\mu$ are Jastrow factors describing the formation of μ -composite bosons ${}^\mu\text{CB}$ (fermions ${}^\mu\text{CF}$) for μ even (odd). We here performed similar MC simulations and calculated the variational energy of hexagonal CWCs for different μ . We take into account only direct but no exchange terms and check that the first exchange corrections are negligible. Our results are shown in fig.3 (a) and we observe that for $\nu \leq 1/6$ CWCs are energetically favorable compared to LN states. We thus expect crystalline order already for $\nu < \nu_{\text{Ld}} = 1/4$ in agreement with the stability analysis and long before the simple NWC becomes energetically favorable at $\nu = \nu_{\text{NWC}}$. More specifically we expect a ${}^4\text{CB}$ CWC ground state at $\nu = 1/6$ and $\nu = 1/8$. For $\nu = 1/10$ the ${}^4\text{CB}$ and ${}^5\text{CF}$ CWCs are equal in energy within our MC errors and we can not make a final conclusion about the underlying CPs.

Our conclusion of crystallization for $\nu \leq 1/6$ is further supported by numerical results for small systems. Using ED in spherical geometry we obtained LN-like states at $a_B = 0.2\ell_B$ for all ν at the accessible particle numbers N , however extrapolation of the gap to collective excitations yields a negative TDL value for $\nu \leq 1/6$. Additionally the second order correlations show strongly enhanced os-

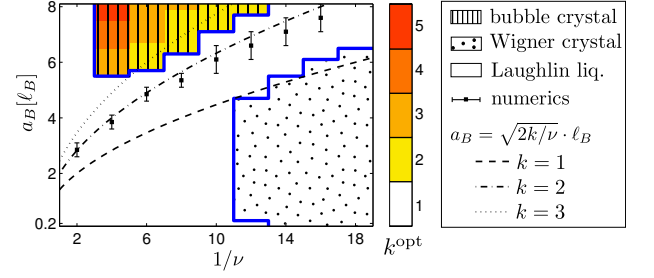


FIG. 4. (color online). Phase diagram (for $1/\nu \in 2\mathbb{N}$) obtained from the comparison of variational energies of LN state ($N = 100$ using Metropolis MC) and bubble crystal. The optimal number k^{opt} of particles per cluster (color code) was used in the BC region. The squares with error bars show the phase transition from LN to a symmetry-breaking state obtained numerically (ED, spherical geometry).

cillations as compared to those expected for LN liquids, while for small r the correlations still decay according to a power law, e.g. $g^{(2)}(r) \sim r^{-11}$ for $N = 6$ at $\nu = 1/8$. This is a direct indication that the ground state physics of these systems is dominated by ${}^\mu\text{CPs}$ with μ between 4 and 6, as predicted by our MC results presented above. More details about these numerical signatures can be found in the supplementary material.

Bubble crystal at large blockade radii. In the following we discuss the effects arising from the competition of the magnetic length ℓ_B with the new length, the blockade radius a_B . Specifically we consider the case where there are more than two particles per blockade area $A_B = \pi a_B^2$, i.e. the regime $a_B \gtrsim \sqrt{2/\nu}\ell_B$. ED results obtained on spheres suitable for LN states show that for $a_B \lesssim \sqrt{2/\nu}\ell_B$, the ground state is a LN state with vanishing angular momentum $L = 0$. For $a_B \approx \sqrt{4/\nu}\ell_B$ a transition to a $L \neq 0$ state is observed, which after mapping from sphere (radius R) to plane (momentum k), $kR = L$ [48], corresponds to a breaking of translational invariance. Fig.3 (b) shows numerical results for the two-particle correlation $g^{(2)}$ for $\nu = 1/2$ and $\nu = 1/4$ for different ratios of a_B/ℓ_B . For small a_B ($L = 0$ phase) we find LN-like correlations while for large a_B ($L \neq 0$ phase) we find particle bunching at $r = 0$, which indicates clustering. Clustering of k particles can also be seen in the $k + 1$ -st-order density correlations,

$$g^{(k+1)}(z) \equiv \left\langle \left(\hat{\Psi}^\dagger(0) \right)^k \hat{\Psi}^\dagger(z) \hat{\Psi}(z) \left(\hat{\Psi}(0) \right)^k \right\rangle.$$

E.g. for $a_B = 2.9\ell_B$, $k = 2$ particles cluster, resulting in a very small $g^{(3)}(0) \approx 2 \times 10^{-5} (\nu/2\pi)^3$ (for $\nu = 1/2$, $N = 8$), while $g^{(2)}(0) = 0.9 (\nu/2\pi)^2$ is still large.

These numerical findings can be explained as follows: For $a_B > \sqrt{4/\nu}\ell_B$ where there are more than two particles per A_B , the long-range contribution to the interaction energy can be reduced by bringing the particles inside A_B together. At the same time there is no energy penalty from interactions inside A_B since the potential

(1) is constant for $r \lesssim a_B$. This provides a pairing mechanism. Assuming that all particles within A_B undergo clustering, one expects a transition from $k-1$ to k particles per cluster at $a_B^{(k)} = \sqrt{2k/\nu} \cdot \ell_B$.

By analogy we expect the formation of a NWC consisting of clusters, when the reduced cluster filling $\nu_{cl} = \nu/k$ is small. This state is referred to as bubble crystal (BC) and was e.g. considered for electrons in a weak magnetic field where $\nu > 1$, i.e. beyond the LLL [49]. The present situation is comparable since the effective interaction in a higher LL is “smeared out” around $r = 0$. A BC phase was also predicted for dipolar bosons at filling $\nu = 1/2$ with large finite-thickness effects [50]. To verify that BCs are indeed good ground state candidates for large blockade radii we calculate the variational energy per particle by generalizing (4). This yields

$$\epsilon_{BC}(k; \nu) = k \cdot \epsilon_{NWC}(\nu = \nu_{cl}) + (k-1) V_0, \quad (5)$$

where the second term describes the binding energy per particle required for the cluster formation. In fig.4 the ground state phase diagram is shown determined by comparing the variational energies of the LN liquid, the NWC and the BC. Also shown are the transition points between symmetry conserving ($L = 0$) and symmetry breaking ($L \neq 0$) states obtained from ED. One recognizes that BC ground states with $k \geq 2$ exist for $\nu \leq 1/4$ and $a_B \gtrsim a_B^{(2)}$.

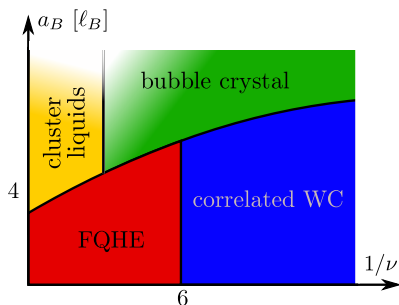


FIG. 5. (color online). Qualitative form of the LLL phase diagram.

Large filling and large a_B : For $\nu = 1/2$ the BC is higher in energy than the LN state for *all* a_B and thus the nature of the ground state for large a_B and large filling is an open question. Besides clustered crystalline states many different correlated cluster *liquids* have been proposed and discussed in the context of the FQHE in higher LLs. Our preliminary studies indicate that in this regime cluster liquid states with exotic properties emerge such as the Haffnian state (Hf) [51]. ED calculations for small systems ($N \leq 10$) suggest that in our system the Hf is an incompressible ground state for $a_B/\ell_B \approx 2.8 \dots 3.5$, which is surprising as it is believed that it describes a compressible state [51]. The arguments used in [51] rely however on the fact that the effective composite interaction is repulsive for all r , and there are good arguments that this may not be the case for the present Rydberg system. Thus this parameter regime, which may be easier accessible experimentally than the low-filling regimes discussed above, is potentially a very interesting one. In order to make more definite statements further studies are needed however.

Summarizing, we have shown that Rydberg-dressed Bose gases can give rise to extremely strong interactions and a variety of interesting correlated phases not found in the standard FQH physics of the LLL. This has two reasons: the rapid fall-off of the interaction potential with distance and the competition of two length scales, a_B and ℓ_B . A qualitative picture of the LLL phase diagram is shown in fig.5. In the limit of pure van-der-Waals interactions ($a_B/\ell_B \rightarrow 0$) the $\nu = 1/2, 1/4$ Laughlin states are exact ground states. Although we mainly discussed filling fractions with even values of $1/\nu$ the entire region is denoted by “FQHE” since we expect the standard bosonic FQH physics [20] to hold for all fractional fillings larger than $\nu = 1/6$. For $\nu \leq 1/6$ we find correlated Wigner crystal ground states, while a noncorrelated Wigner crystal ansatz predicts crystallization only at $\nu = 1/12$. For $a_B \gtrsim \sqrt{4/\nu} \ell_B$ and $\nu \leq 1/4$ a transition to a bubble crystal is expected. Finally, for larger fillings and blockade radii the nature of the ground state is an open question, and for filling $\nu = 1/2$ we speculated on a connection to cluster liquid states in particular the Haffnian [51].

We thank J. Otterbach for helpful discussions and M. Baranov for drawing our attention to the crystal stability analysis. F.G. acknowledges financial support from the the Graduate School of Excellence MAINZ.

-
- [1] B. I. Halperin, Physical Review Letters **52**, 1583 (1984)
 - [2] D. Arovas, J. R. Schrieffer, and F. Wilczek, Physical Review Letters **53**, 722 (1984)
 - [3] G. Moore and N. Read, Nuclear Physics B **360**, 362 (Aug. 1991)
 - [4] C. Nayak and F. Wilczek, Nuclear Physics B **479**, 529 (Nov. 1996)
 - [5] P. Bonderson, V. Gurarie, and C. Nayak, Physical Review B **83**, 075303 (Feb. 2011)
 - [6] A. Y. Kitaev, Annals of Physics **303**, PII S0003 (Jan. 2003)
 - [7] C. Nayak, S. H. Simon, A. Stern, M. Freedman, and S. Das Sarma, Reviews of Modern Physics **80**, 1083 (Jul. 2008)
 - [8] D. J. Thouless, M. Kohmoto, M. P. Nightingale, and M. denNijs, Physical Review Letters **49**, 405 (1982)
 - [9] N. R. Cooper, N. K. Wilkin, and J. M. F. Gunn, Physical Review Letters **87**, 120405 (Sep. 2001)

- [10] N. R. Cooper, *Advances In Physics* **57**, PII 906577892 (2008)
- [11] A. L. Fetter, *Reviews of Modern Physics* **81**, 647 (Apr. 2009)
- [12] G. Juzeliunas and P. Ohberg, *Physical Review Letters* **93**, 033602 (Jul. 2004)
- [13] J. Dalibard, F. Gerbier, G. Juzeliunas, and P. Oehberg, *Reviews of Modern Physics* **83** (Nov. 2011),
- [14] Y. . J. Lin, R. L. Compton, K. Jimenez-Garcia, J. V. Porto, and I. B. Spielman, *Nature* **462**, 628 (Dec. 2009)
- [15] K. W. Madison, F. Chevy, W. Wohlleben, and J. Dalibard, *Physical Review Letters* **84**, 806 (Jan. 2000)
- [16] J. R. Abo-Shaeer, C. Raman, J. M. Vogels, and W. Ketterle, *Science* **292**, 476 (Apr. 2001)
- [17] V. Schweikhard, I. Coddington, P. Engels, V. P. Moggendorff, and E. A. Cornell, *Physical Review Letters* **92**, 040404 (Jan. 2004)
- [18] N. K. Wilkin, J. M. F. Gunn, and R. A. Smith, *Physical Review Letters* **80**, 2265 (Mar. 1998)
- [19] N. R. Cooper and N. K. Wilkin, *Physical Review B* **60**, 16279 (1999)
- [20] N. Regnault and T. Jolicoeur, *Physical Review Letters* **91**, 030402 (Jul. 2003)
- [21] K. Osterloh, N. Barberan, and M. Lewenstein, *Physical Review Letters* **99**, 160403 (Oct. 2007)
- [22] M. A. Baranov, K. Osterloh, and M. Lewenstein, *Physical Review Letters* **94**, 070404 (Feb. 2005)
- [23] E. H. Rezayi, N. Read, and N. R. Cooper, *Physical Review Letters* **95**, 160404 (Oct. 2005)
- [24] R. B. Laughlin, *Physical Review Letters* **50**, 1395 (1983)
- [25] D. Tong, S. M. Farooqi, J. Stanojevic, S. Krishnan, Y. P. Zhang, R. Cote, E. E. Eyler, and P. L. Gould, *Physical Review Letters* **93**, 063001 (Aug. 2004)
- [26] K. Singer, M. Reetz-Lamour, T. Amthor, L. G. Marcassa, and M. Weidemuller, *Physical Review Letters* **93**, 163001 (Oct. 2004)
- [27] T. Vogt, M. Viteau, J. Zhao, A. Chotia, D. Comparat, and P. Pillet, *Physical Review Letters* **97**, 083003 (Aug. 2006)
- [28] R. Heidemann, U. Raitzsch, V. Bendkowsky, B. Butscher, R. Low, L. Santos, and T. Pfau, *Physical Review Letters* **99**, 163601 (Oct. 2007)
- [29] R. Heidemann, U. Raitzsch, V. Bendkowsky, B. Butscher, R. Low, and T. Pfau, *Physical Review Letters* **100**, 033601 (Jan. 2008)
- [30] M. Viteau, M. G. Bason, J. Radogostowicz, N. Malossi, D. Ciampini, O. Morsch, and E. Arimondo, *Physical Review Letters* **107**, 060402 (Aug. 2011)
- [31] A. Schwarzkopf, R. E. Sapiro, and G. Raithel, *Physical Review Letters* **107**, 103001 (Aug. 2011)
- [32] N. Henkel, R. Nath, and T. Pohl, *Physical Review Letters* **104**, 195302 (May 2010)
- [33] J. E. Johnson and S. L. Rolston, *Physical Review A* **82**, 033412 (Sep. 2010)
- [34] C. G. Darwin, *Proceedings of the Cambridge Philosophical Society* **27**, 86 (Sep. 1931)
- [35] N. Henkel, F. Cinti, P. Jain, G. Pupillo, and T. Pohl, *Physical Review Letters* **108**, 265301 (Jun. 2012)
- [36] F. D. M. Haldane, *Physical Review Letters* **51**, 605 (1983)
- [37] K. Maki and X. Zotos, *Physical Review B* **28**, 4349 (1983)
- [38] P. K. Lam and S. M. Girvin, *Physical Review B* **30**, 473 (1984)
- [39] M. A. Baranov, H. Fehrmann, and M. Lewenstein, *Physical Review Letters* **100**, 200402 (May 2008)
- [40] N. Metropolis, A. W. Rosenbluth, M. N. Rosenbluth, A. H. Teller, and E. Teller, *Journal of Chemical Physics* **21**, 1087 (1953)
- [41] W. Pan, H. L. Stormer, D. C. Tsui, L. N. Pfeiffer, K. W. Baldwin, and K. W. West, *Physical Review Letters* **88**, 176802 (Apr. 2002)
- [42] H. Fukuyama, *Solid State Communications* **19**, 551 (1976)
- [43] Y. E. Lozovik and V. M. Farztdinov, *Solid State Communications* **54**, 725 (1985)
- [44] J. K. Jain, *Physical Review Letters* **63**, 199 (Jul. 1989)
- [45] H. M. Yi and H. A. Fertig, *Physical Review B* **58**, 4019 (Aug. 1998)
- [46] C. C. Chang, G. S. Jeon, and J. K. Jain, *Physical Review Letters* **94**, 016809 (Jan. 2005)
- [47] It can be concluded from plasma analogy [45] that the lattice constant a used for the NWC in the definition of the CWC wavefunction have to be rescaled in order to produce the desired density at filling ν : $a \rightarrow a(1 - \mu \cdot \nu)$.
- [48] F. D. M. Haldane, In "The Quantum Hall Effect", ed. R. E. Prange and S. M. Girvin (New York: Springer, 1990)
- [49] A. A. Koulakov, M. M. Fogler, and B. I. Shklovskii, *Physical Review Letters* **76**, 499 (Jan. 1996)
- [50] N. R. Cooper, E. H. Rezayi, and S. H. Simon, *Physical Review Letters* **95**, 200402 (Nov. 2005)
- [51] D. Green, *Strongly Correlated States in Low Dimensions*, Ph.D. thesis, Yale University (2001)

Supplementary Material for "Fractional quantum Hall physics in rotating ultracold Rydberg gases"

F. Grusdt and M. Fleischhauer

I. PSEUDOPOTENTIALS AND ENERGY SCALES

In disc geometry the Haldane pseudopotentials are given by

$$V_m = \frac{1}{2^{2m+1}m!} \int_0^\infty dr r^{1+2m} V(r) e^{-r^2/4}, \quad (6)$$

where for bosons (fermions) only $m = 0, 2, 4, \dots$ ($m = 1, 3, 5, \dots$) are relevant. In fig. 1(b) of the main text we plotted $V_{0,2,4,\dots}(a_B)$ together with contour lines of the continuous function $V(m) \equiv V_m$ for $m \in \mathbb{R}$ defined as in (6) above. Table I lists some explicit values of V_m . The characteristic energy scales for Rydberg-Rydberg interactions are limited by demanding LLL-approximation (i.e. $V_0 \ll \hbar\omega_c$), different from all previously discussed interactions in cold gases. This is due to the large values V_0 may take, as can be seen from tables II and III for Rb. There we assume a fixed magnetic length $\ell_B \approx 1\mu\text{m}$ (corresponding to $\omega_c \approx 2\pi \cdot 130\text{Hz}$ which is a realistic value [1]) as well as a fixed ratio $\Omega/\Delta = 0.1$. For the $60S_{1/2}$ Rydberg state in Rb, $C_6(n=60)/2\pi = 0.14\text{THz}\mu\text{m}^6$ and we used the scaling law $C_6(n) \propto n^{11}$ [2]. In table II $\Delta = 2\pi \cdot 1\text{GHz}$ is constant and the principle quantum number of the Rydberg state n is varied. In table III on the other hand, $n = 46$ is fixed and the detuning Δ is varied. Note that in the latter case it is even possible to tune the interaction potential adiabatically.

a_B/ℓ_B	$V_0[\tilde{C}_6/\ell_B^6]$	V_2/V_0	V_4/V_0	V_6/V_0	V_8/V_0	V_{10}/V_0	V_{12}/V_0	V_{14}/V_0
0.1	$3.015 \cdot 10^3$	$1.40 \cdot 10^{-5}$	$2.16 \cdot 10^{-7}$	$4.30 \cdot 10^{-8}$	$1.54 \cdot 10^{-8}$	$7.19 \cdot 10^{-9}$	$3.91 \cdot 10^{-9}$	$2.37 \cdot 10^{-9}$
0.2	$1.871 \cdot 10^2$	$1.69 \cdot 10^{-4}$	$3.48 \cdot 10^{-6}$	$6.95 \cdot 10^{-7}$	$2.49 \cdot 10^{-7}$	$1.16 \cdot 10^{-7}$	$6.31 \cdot 10^{-8}$	$3.82 \cdot 10^{-8}$
0.3	$3.652 \cdot 10^1$	$6.93 \cdot 10^{-4}$	$1.78 \cdot 10^{-5}$	$3.56 \cdot 10^{-6}$	$1.27 \cdot 10^{-6}$	$5.95 \cdot 10^{-7}$	$3.23 \cdot 10^{-7}$	$1.96 \cdot 10^{-7}$
1	$2.455 \cdot 10^{-1}$	$3.43 \cdot 10^{-2}$	$2.53 \cdot 10^{-3}$	$5.28 \cdot 10^{-4}$	$1.89 \cdot 10^{-4}$	$8.82 \cdot 10^{-5}$	$4.80 \cdot 10^{-5}$	$2.91 \cdot 10^{-5}$
2	$9.816 \cdot 10^{-3}$	0.223	$4.56 \cdot 10^{-2}$	$1.24 \cdot 10^{-2}$	$4.66 \cdot 10^{-3}$	$2.20 \cdot 10^{-3}$	$1.20 \cdot 10^{-3}$	$7.28 \cdot 10^{-4}$
3	$1.172 \cdot 10^{-3}$	0.505	0.203	$8.06 \cdot 10^{-2}$	$3.55 \cdot 10^{-2}$	$1.77 \cdot 10^{-2}$	$9.91 \cdot 10^{-3}$	$6.04 \cdot 10^{-3}$
4	$2.314 \cdot 10^{-4}$	0.740	0.450	0.250	0.137	$7.75 \cdot 10^{-2}$	$4.63 \cdot 10^{-2}$	$2.92 \cdot 10^{-2}$
5	$6.279 \cdot 10^{-5}$	0.877	0.680	0.479	0.322	0.212	0.140	$9.47 \cdot 10^{-2}$
10	$9.996 \cdot 10^{-7}$	0.996	0.987	0.970	0.944	0.908	0.863	0.811

TABLE I. Leading order bosonic (m even) pseudopotentials V_m for the potential $V(r) = \tilde{C}_6/(r^6 + a_B^6)$ from the main text.

n	40	50	60	70	80	90	100
$a_B [\mu\text{m}]$	0.97	1.5	2.0	2.7	3.4	4.3	5.2
$V_0/2\pi [\text{kHz}]$	2.8	5.3	7.9	9.9	11.2	11.8	12.1

TABLE II. Realistic blockade radii a_B and energies V_0 for Rb with $\omega_c \approx 2\pi \cdot 130\text{Hz}$ (i.e. $\ell_B \approx 1\mu\text{m}$), $\Delta = 10\Omega = 2\pi \cdot 1\text{GHz}$ as a function of the principle quantum number n .

$\Delta[\text{MHz}]$	1.0	3.0	9.0	30	80	250	700	$2.0 \cdot 10^3$	$6.5 \cdot 10^3$	$20 \cdot 10^3$
$a_B [\mu\text{m}]$	3.94	3.28	2.73	2.24	1.90	1.57	1.32	1.11	0.91	0.76
$V_0/2\pi [\text{kHz}]$	0.0744	0.210	0.574	1.65	3.75	9.37	20.8	45.7	107.8	240.0

TABLE III. Realistic blockade radii a_B and energies V_0 for Rb with $\omega_c \approx 2\pi \cdot 130\text{Hz}$ (i.e. $\ell_B \approx 1\mu\text{m}$), $n = 46$ as a function of the detuning of the dressing laser Δ . Note that the Rabi frequency Ω was chosen as $\Omega = 0.1\Delta$.

II. EXACT DIAGONALIZATION

In addition to variational calculations we performed state-of-the-art exact diagonalization (ED) studies. To

minimize the role of finite-size effects we did all our systematic investigations in spherical geometry. We work on standard desktop computers and have excess up to the following particle numbers:

ν	1	1/2	1/4	1/6	1/8
N_{\max}	14	10	7	6	6
dim.	194668	246448	48417	32134	118765

The dimension of the full Hilbertspace containing all angular momentum multiplets is given, since we do not explicitly exploit that $[\mathcal{H}, \vec{L}_{\text{tot}}^2] = 0$ in the numerics. In the numerics the filling fraction ν is adjusted by changing the magnetic flux N_Φ through the surface of the sphere. For $\nu = 1/2, 1/4, \dots$ Laughlin states

$$N_\Phi = \frac{N-1}{\nu}.$$

We eliminate leading-order finite size effects by rescaling the magnetic length [3],

$$\ell_B \rightarrow \ell_B^\infty = \sqrt{\frac{N_\Phi \nu}{N}} \ell_B.$$

In simulations a_B must be chosen small enough since when the blockade area fills half a sphere, i.e. when $a_B \geq \pi\sqrt{N_\Phi}/8\ell_B$, we expect the formation of two clusters on opposite poles. We indeed found large overlaps to two-cluster trial wavefunctions in this case and no conclusions about the thermodynamic limit can be drawn.

In disc geometry we only performed systematic studies for small $a_B \lesssim \ell_B$ and found similar results as in spherical geometry. The accessible system sizes are the same as above, although requiring slightly more CPU time.

III. NUMERICAL RESULTS AT $\nu = 1/6, 1/8$

In the main text we summarized the most important numerical indications for crystallization at $\nu = 1/6, 1/8$ and for small $a_B \lesssim \ell_B$. Here we give further details about these ED calculations in spherical geometry. We obtain substantial overlaps to Laughlin (LN) states for small systems, see table IV. Besides a region of almost zero overlap (large a_B) we find that for $\nu = 1/6$ LN states describe the ground state much worse than for $\nu = 1/2, 1/4$. In the main text we stated that for $\nu = 1/6, 1/8$ finite-size extrapolations yield negative gaps to collective excitations. This can be seen in fig. 6 (a). The results for $\nu = 1/4$ are shown for comparison, and they clearly yield a positive gap in thermodynamic limit. The gap ΔE was obtained as the difference from ground to first excited state. The latter can well be described as a density wave and exhibits a roton minimum [4, 5]. Vanishing $\Delta E \rightarrow 0$ thus signals an instability with respect to crystallization.

In fig. 6 (b) second order correlations are shown for $\nu = 1/8$ and $a_B = 0.2\ell_B$. As mentioned in the main text, we find strongly enhanced oscillations for $N = 6$ signaling a trend towards long-range order. For $N = 5$ this effect is absent, which can be attributed to a more general finite-size effect: Already for the gaps (fig. 6 (a)) we observe a different behavior for N even/odd at $\nu = 1/6, 1/8$. For $N = 2, 4, 6$, ΔE is smaller than for

$N = 3, 5$ and we find the same behavior for the ground state energy. This is another indication for crystallization, since also for a classical vdW crystal on a sphere the ground state energy per particle shows these oscillations [?]. The system is thus expected to be more susceptible to density modulations for even N . This in turn explains (i) the smaller gap and (ii) the enhanced oscillations of the ground state correlations at $N = 2, 4, 6$. For $\nu = 1/4$ this finite-size effect is not observed, fully consistent with our result (see main text) that crystallization takes place only for $\nu < 1/4$. Finally we note that the discussed finite-size effect is due to incommensurability but not due to pairing since the latter would imply large $g^{(2)}(0)$ but small $g^{(3)}(0)$ which we do not observe.

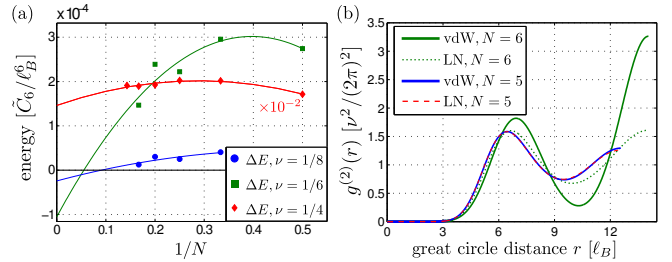


FIG. 6. (color online). (a) Gap to collective excitations ΔE at $\nu = 1/4, 1/6, 1/8$ and for $a_B = 0.2\ell_B$. Note that for $\nu = 1/4$ energies were scaled down by a factor of 100. ED in spherical geometry was used and finite-size corrections were performed as described in sec. II. Solid lines: quadratic fits. (b) Second order correlation functions of the ground state for van-der-Waals (vdW) interactions at $a_B = 0.2\ell_B$ and $\nu = 1/8$, compared to those of the LN liquids at the corresponding system size. ED in spherical geometry was used.

a_B/ℓ_B	$\nu = 1/2$	$\nu = 1/4$	$\nu = 1/6$
5.6	$1.051 \cdot 10^{-09}$	$4.743 \cdot 10^{-21}$	$4.179 \cdot 10^{-12}$
5.1	$4.935 \cdot 10^{-10}$	$1.079 \cdot 10^{-15}$	$1.682 \cdot 10^{-14}$
4.6	$2.491 \cdot 10^{-10}$	$3.410 \cdot 10^{-08}$	0.6988
4.1	$7.303 \cdot 10^{-10}$	$3.668 \cdot 10^{-29}$	0.7298
3.6	$6.074 \cdot 10^{-09}$	0.8536	0.7592
3.1	$2.594 \cdot 10^{-03}$	0.9026	0.7962
2.6	0.9678	0.9403	0.8371
2.1	0.9940	0.9696	0.8757
1.6	0.9985	0.9876	0.9058
1.1	0.9998	0.9960	0.9239
0.6	0.999995	0.9990	0.9311
0.1	0.999999999978	0.99988	0.9320

TABLE IV. Overlaps squared of the ground state to the Laughlin states at fillings $\nu = 1/2, 1/4, 1/6$. Both were obtained using ED at $N = 6$ in spherical geometry.

-
- [1] V. Bretin, S. Stock, Y. Seurin, and J. Dalibard, Physical Review Letters **92**, 050403 (Feb. 2004)
- [2] K. Singer, J. Stanojevic, M. Weidemuller, and R. Cote, Journal of Physics B-atomic Molecular and Optical Physics **38**, S295 (Jan. 2005)
- [3] N. Dambrumenil and R. Morf, Physical Review B **40**, 6108 (Sep. 1989)
- [4] S. Girvin, A. H. MacDonald, and P. Platzman, Physical Review B **33**, 2481 (1986)
- [5] R. K. Kamilla, X. G. Wu, and J. K. Jain, Physical Review Letters **76**, 1332 (Feb. 1996)
- [6] The ground state energy can easily be calculated for a given configuration. For small particle numbers on the sphere, the problem of finding the ground state configuration is known as Thomson's problem and it is still not completely solved, see <http://arxiv.org/abs/1001.3702>.